Shahrood University of Technology

Journal of Mining and Environment (JME)

Journal homepage: www.jme.shahroodut.ac.ir

Iranian Society of Mining Engineering (IRSME)

Formulation of a Bearing Capacity Equation for a Circular Footing with Vertical and Inclined Loads on Layered Sand

Surya Pratap Singh* and Amrit Kumar Roy

Civil Engineering Department, NIT Hamirpur, Himachal Pradesh, India

Article Info

Received 9 October 2022

Received in Revised form 30 October 2022

Accepted 11 November 2022

Published online 11 November 2022

DOI:10.22044/jme.2022.12332.2238

Keywords

Circular footing

Projected area approach

Vertical and inclined loading

Layered sand

Abstract

This research work provides a bearing capacity equation for a circular footing placed on dense sand overlying loose sand and subjected to vertical and inclined loading, utilizing the limit equilibrium followed by the projected area approach. For the parametric study, the variables include upper dense sand layer thickness ratio (0.5 to 2.00), friction angle of upper dense sand (41° to 45°) and lower loose sand layer (31° to 35°), and applied load inclination (0° to 30°). The highest and lowest increases in bearing capacity are reported for friction angle combinations of 45°–35° and 41°–31° for various thickness ratios, respectively. For load inclinations of 0°, 10°, 20°, and 30°, bearing capacity is reduced by 43.51%, 72.17%, 85.64%, and 22.62%, 48.56%, 62.17% for friction angles of upper dense and lower loose sand layer combinations of 45° and 35° and at a thickness ratio of 0.5 and 2.0. Considering finite element results, the average deviation of the bearing capacity derived from the suggested equation at surface footing is 7%, 5%, 22%, and 23% for 0°, 10°, 20°, and 30° load inclinations, respectively. The proposed bearing capacity equation yield results that are compared with the available literature, with average deviations of 62%, 50%, 36%, and 36% for load inclination values of 0°, 10°, 20°, and 30°, respectively.

1. Introduction

The superstructure's load is transferred to the soil beneath it via the footing. A footing's depth-to-width ratio defines whether it is shallow or deep. The load must be transferred beneath the footing in such a way that settling and shear failure are avoided. The behaviour of footings in layered soils is extremely complex and has been a source of concern for decades. Several researchers investigated the behaviour of footings in homogenous soft soils, and several design approaches were created to determine the eventual bearing capacity. The researchers have documented a number of studies in the literature [1-4].

The majority of bearing capacity calculations found in the literature assumes homogeneous soil deposits beneath the footing base. However, in actuality, soil mass is heterogeneous and anisotropic. The problem of determining the ultimate bearing capacity can be solved by utilising the analytical and experimental methods. In the analytical method, the plasticity theory and finite elements can be utilised, but in the experimental method, many types of models and prototypes can be explored.

Evaluate the bearing capacity of footings subjected to vertical or inclined loads on single layer or layered soils [5] [6] [7].Under vertical load, the researchers examined the bearing capacity of strip and circular footings on layered soil (dense sand over loose sand) [8-10].

The vertical load bearing capacity of the strip footing, the circle footing, and the square/rectangular footing on the layered soil (dense sand over soft clay, stiff clay over soft clay, stiff over soft clay, stiff over loose sand) was evaluated [1] [11-15].

The limit equilibrium method was used to determine the bearing capacity of the strip and circular footings under vertical and inclined loads.

Corresponding author: surya_phdce@nith.ac.in (S. Pratap Singh).

Using the punched shear coefficient for vertical and inclined loading, an equation was proposed for the ultimate bearing capacity of strip and circular footings on layered soil (dense sand over loose sand). However, the findings of were overestimates the bearing capacity at greater depths [1] [2] [16] [17].

Estimate the bearing capacity of strip, circular, and square or rectangular footings on layered soil under vertical loading using the projected area method [11]. In order to predict the ultimate bearing capacity for strip, circular, and square/rectangular footings on layered soil (dense sand over soft clay) using punching shear coefficients, load dispersion angles, and soil properties under vertical loading, it was found that a proposed equation overestimated the bearing capacity in comparison to previous studies [18] [14] [19].

Recent finite element modelling has been utilised to evaluate the bearing capacity of strip, circular, square, and rectangular footings over layered soil (dense sand over loose sand, dense sand over soft clay, soft clay over dense sand, and soft clay over stiff clay) [13] [8] [20-22].

This work focuses on the fact that no equation of ultimate bearing capacity for circular footings subjected to vertical and inclined loads has been published, particularly for layered soils (dense sand over loose sand). Consequently, utilising the punching shear mechanism and limit equilibrium approach, the current work derived an equation for the bearing capacity of circular footings on dense sand overlying loose sand under vertical and inclined loading. Using finite element analysis, the load distribution mechanism in the upper dense sand layer was chosen to obtain an accurate estimate of bearing capacity. The bearing capacity of the circular footing over layered sand was computed for different friction angles of the upper dense and lower loose sand layers, load inclination, and different upper dense sand layer thicknesses at the surface footing. The results obtained were compared to those in the scientific literature.

2. Methodology

As shown in Figure 1., the bearing capacity of a circular foundation is analysed. The footing has a radius of r_1 (or a diameter of D), and H is the distance from the base of the footing to the interface between dense and loose sand. The various soil properties for dense sand and loose sand are Υ_1, ϕ_1, and Υ_2, ϕ_2 respectively. The assumption was that the load from the footing would spread through the upper dense sand to the lower loose sand.

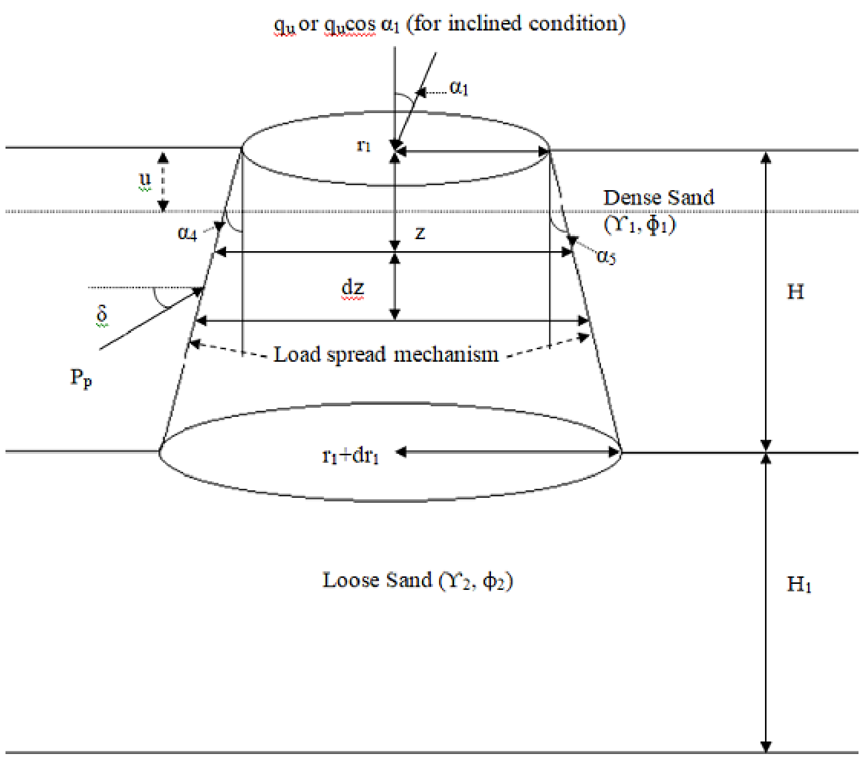

Figure 1. Assumed failure surface for circular footing under vertical and inclined loading.

The footing is placed on the soil surface and the embedded depth of the footing is considered as 'u' in the equation. It was assumed that the passive pressure (Pp) acted on the failure surface at an angle of normal to the failure surface. It was assumed that the failure occurred at the interface between the upper dense and lower loose sand layers. Figure 1.shows a plan view of the assumed punched shear failure mechanism, followed by the projected area approach under vertical and inclined loading (q_u) for the circular footing with load dispersion angles of α_2 and α_3 across and α_4 and α_5 along the diameter of the footing. The following are the assumptions made for mathematical derivation.

1. It is considered that the upper dense sand layer of the footing provides a rigid and rough base.
2. It is assumed that the sand layers meet the ground at a horizontal interface.
3. The water table effect on the circular footing ultimate bearing capacity was ignored in the study. The water table was predicted to be located far below the layer of loose sand below it.
4. With a friction angle of ϕ_1 for the upper dense sand layer and ϕ_2 for the lower loose sand layer, both should have been completely drained.
5. It is assumed that over the failure surface, the shear strength of both the top dense sand and the lower loose sand is fully mobilised.
6. According to [2], passive pressure is assumed to be constant around the entire modelled region.
7. In the middle of the circular footing, a load (q_u) is acting at an angle of load inclination (α_1).

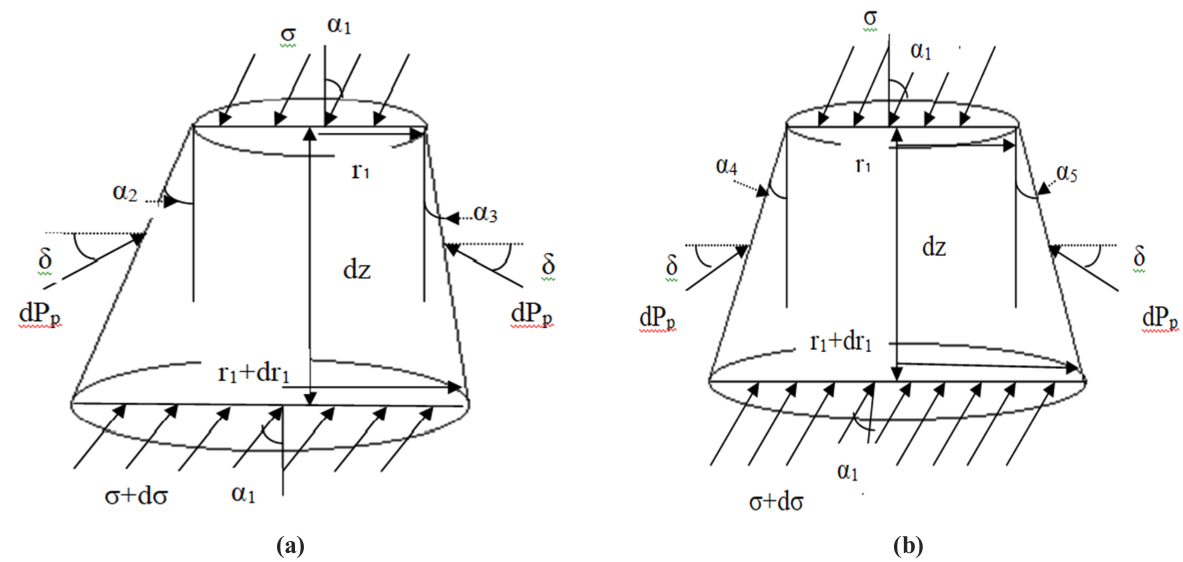

Figure 2. Under vertical and inclined loading, the diagram shows the stress distribution along and across the diameter.

In addition, a frustum of thickness dz is considered in the analysis, as illustrated in Figure 2, at a distance z from the centre of the circular footing. Figure 2. depicts the numerous forces that were taken into account during the analysis of this frustum. Total passive earth pressure (Pp) acts on the punching surface create by the circular footing in dense sand, and this pressure is dP_{pv} at an angle δ to the horizontal as it acts on the curving surface of the frustum of thickness dz. The concept of passive pressure being inclined originates from the fact that it effectively resists the load that is being applied to the soil by the foundation. The vertical force exerted on the top and bottom of a dz-thick frustum is denoted by σ and $\sigma+d\sigma$, respectively. The frustum with a thickness of dz exerts a downward force due to its own self-weight.

According to the limit equilibrium concept, the total upward-pointing force is assumed to be zero.

$\Sigma F_v=0$

$$\sigma(\pi r_1^2) - (\sigma + d\sigma) \times \pi(r_1 + dr_1)^2 - dP_{pv} + \gamma_1 \pi dz \frac{(3r_1^2 + dr_1^2 + 3r_1\, dr_1)}{3} = 0 \quad (1)$$

where, γ_1 is the unit weight of dense sand in the thickness dz frustum

dP_p in vertical direction is $dP_{pv}\sin\delta$

$dP_{pv} = dP_p\ (Sin\ \delta)$

$$dP_{pv} = K_p\gamma_1\left(u + z + \frac{dz}{2}\right)\Big[\frac{\pi}{4}(2r_1 + dr_1)dz\ Sec\ \alpha_2 + \frac{\pi}{4}(2r_1 + dr_1)dz\ Sec\ \alpha_3 + \frac{\pi}{2}(2r_1 + dr_1)dz\ Sec\ \alpha_4\Big]\ Sin\ \delta$$

Expanding Equation (1) and neglecting the smaller quantities such as $-\sigma\pi dr_1^2$, $-d\sigma\pi dr_1^2$, $-d\sigma 2\pi r_1 dr_1$, $\gamma_1\pi dz\ dr_1^2/3$, $\gamma_1\pi dz r_1\ dr_1$. As $d\sigma$, dr_1, dz were small quantities, the product or square of these quantities was very small as a result of Equation (2).

$$(\pi r_1^2) - (\sigma + d\sigma)(\pi r_1^2 + \pi dr_1^2 + 2\pi r_1 dr_1) - dP_{pv} + \frac{(3r_1^2\ \gamma_1\pi dz + \gamma_1\pi dz\ dr_1^2 + 3r_1\ dr_1\gamma_1\pi dz)}{3} = 0$$

$$-\sigma(2\pi r_1 dr_1) - d\sigma\pi r_1^2 - dP_{pv} + r_1^2\ \gamma_1\pi dz = 0 \quad (2)$$

Putting the value of $dP_{pv}sin\delta$ in Equation (2), solving and neglecting the smaller quantities $K_p\gamma_1 udr_1$ dz $sec\alpha_1$ $sin\delta/4$, $K_p\gamma_1 zdr_1$ dz $sec\alpha_1$ $sin\delta/4$, $K_p\gamma_1 udr_1$ dz^2 $sec\alpha_1$ $sin\delta/8$, $K_p\gamma_1 udr_1$ dz $sec\alpha_2$ $sin\delta/4$, $K_p\gamma_1 zdr_1$ dz $sec\alpha_2$ $sin\delta/4$, $K_p\gamma_1 udr_1$ dz^2 $sec\alpha_2$ $sin\delta/8$, $K_p\gamma_1 udr_1$ dz $sec\alpha_3$ $sin\delta/2$, $K_p\gamma_1 zdr_1$ dz $sec\alpha_3$ $sin\delta/2$, $K_p\gamma_1 udr_1$ dz^2 $sec\alpha_3$ $sin\delta/4$. As dr_1, dz were small quantities, the product or square of these quantities was very small as a result of Equation (3).

$$-\sigma(2\pi r_1 dr_1) - d\sigma\pi r_1^2 - \left[\frac{2K_p\gamma_1\pi r_1}{4}udz\ Sec\ \alpha_2 + \frac{2K_p\gamma_1\pi r_1}{4}udz\ Sec\ \alpha_3 + \frac{2K_p\gamma_1\pi r_1}{2}udz\ Sec\ \alpha_4\right]Sin\ \delta - \left[\frac{2K_p\gamma_1\pi r_1}{4}zdz\ Sec\ \alpha_2 + \frac{2K_p\gamma_1\pi r_1}{4}zdz\ Sec\ \alpha_3 + \frac{2K_p\gamma_1\pi r_1}{4}zdz\ Sec\ \alpha_4\right]Sin\ \delta + \gamma_1\pi r_1^2 dz = 0 \quad (3)$$

Dividing Equation (3) by πr_1^2, results in Equation (4).

$$\frac{-2\sigma dr_1}{r_1} - d\sigma - \left[\frac{K_p\gamma_1 u}{2r_1}dz\ Sec\ \alpha_2 + \frac{K_p\gamma_1 u}{2r_1}dz\ Sec\ \alpha_3 + \frac{K_p\gamma_1 u}{2r_1}dz\ Sec\ \alpha_4\right]Sin\ \delta - \left[\frac{K_p\gamma_1 z}{2r_1}dz\ Sec\ \alpha_2 + \frac{K_p\gamma_1 z}{2r_1}dz\ Sec\ \alpha_3 + \frac{K_p\gamma_1 z}{2r_1}dz\ Sec\ \alpha_4\right]Sin\ \delta + \gamma_1 dz = 0 \quad (4)$$

Neglecting the smaller quantities from Equation (4), $-2\sigma dr_1/r_1$ and rewriting the Equation (5) since r_1 is greater than dr_1, the term dr_1/r_1 is very less and the product of dr_1/r_1 and -2σ is also very less compared to the other terms in Equation (5), so it can be ignored.

$$-d\sigma - \frac{K_p\gamma_1 z}{2r_1}dz\ Sin\ \delta\ [Sec\ \alpha_2 + Sec\ \alpha_3 + Sec\ \alpha_4] - \frac{K_p\gamma_1 u}{2r_1}dz\ Sin\ \delta\ [Sec\ \alpha_2 + Sec\ \alpha_3 + Sec\ \alpha_4] + \gamma_1 dz = 0 \quad (5)$$

Indefinite integrating of Equation (5)

$$\sigma = -\frac{K_p\gamma_1 z^2}{2r_1}\ Sin\ \delta\ [Sec\ \alpha_2 + Sec\ \alpha_3 + Sec\ \alpha_4] - \frac{K_p\gamma_1 uz}{2r_1}\ Sin\ \delta\ [Sec\ \alpha_2 + Sec\ \alpha_3 + Sec\ \alpha_4]\ \gamma_1 dz + c \quad (6)$$

where c is integration constant and value of c is determined by applying the boundary condition in Equation (6)

1. At $\sigma = q_u$, $z = 0$, $r_1 = D/2$, putting the values in Equation (6)

   $C = q_u$ or $q_u.cos\alpha_1$

   where, q_u or $q_u.cos\alpha_1$ is the ultimate load bearing capacity of the circular footing in the layered sand.

2. At $\sigma = q_b$ or $q_b.\ cos\alpha_1$, $z = H$, $r_1 = D/2+H(tan\alpha_2+tan\alpha_2+2tan\alpha_3)$, putting the values in Equation (6) result in Equation (7).

$$q_u = q_b + K_p\gamma_1 H^2 \,Sin\,\delta \left[\frac{1}{D\,Cos\,\alpha_2 + 2H\,Sin\,\alpha_2} + \frac{1}{D\,Cos\,\alpha_3 + 2H\,Sin\,\alpha_3} + \frac{1}{D\,Cos\,\alpha_4 + 2H\,Sin\,\alpha_4}\right] + K_p\gamma_1 uH\,Sin\,\delta \left[\frac{1}{D\,Cos\,\alpha_2 + 2H\,Sin\,\alpha_2} + \frac{1}{D\,Cos\,\alpha_3 + 2H\,Sin\,\alpha_3} + \frac{1}{D\,Cos\,\alpha_4 + 2H\,Sin\,\alpha_4}\right] - \gamma_1 H \quad (7)$$

where, q_b or $q_b.\cos\alpha_1$ is the bearing capacity of the lower loose sand layer. $q_u.\cos\alpha_1$ and $q_b.\cos\alpha_1$ is the vertical component of the bearing capacity q_u and q_b respectively in the derivation. The bearing capacity of the lower loose sand layer is calculated by using the IS code- 6403 (1981).

$$q_b = \gamma_1(u + H)N_{q_2}S_{q_2}d_{q_2}i_{q_2} + 0.5\gamma_2 DN_{\gamma_2}S_{\gamma_2}d_{\gamma_2}i_{\gamma_2} \quad (8)$$

where, γ_1 and γ_2 is the unit weight of the upper and lower sand layer, u embedded depth of the footing (if applied), N_{q2}, $N_{\gamma2}$, S_{q2}, $S_{\gamma2}$, d_{q2}, $d_{\gamma2}$ and i_{q2}, $i_{\gamma2}$ were bearing capacity factors, shape, depth and inclination factors. As per (23), the values of N_{q2}, $N_{\gamma2}$ are given in the code remaining factors values are as follow:

$$S_{q_2} = 1.2$$

$$S_{\gamma_2} = 0.6$$

$$d_{q_2} = d_{\gamma_2} = 1 + 0.1\frac{D_f}{D}\sqrt{N_\varphi}$$

$$i_{q_2} = (1 - \frac{\alpha_1}{90^\circ})^2$$

$$i_{\gamma_2} = (1 - \frac{\alpha_1}{\varphi_2})^2$$

for circular footing

Further simplification and rearranging Equation (7) result in Equation (9).

$$q_u = q_b + K_p\gamma_1 H\,Sin\,\delta \left[\frac{1}{D\,Cos\,\alpha_2 + 2H\,Sin\,\alpha_2} + \frac{1}{D\,Cos\,\alpha_3 + 2H\,Sin\,\alpha_3} + \frac{2}{D\,Cos\,\alpha_4 + 2H\,Sin\,\alpha_4}\right](H + u) - \gamma_1 H \quad (9)$$

The ultimate bearing capacity (q_u) calculated according to Equation (9) is only valid up to the bearing capacity of the upper sand layer, after which the bearing capacity remains constant and is mostly dependent on the upper dense sand layer. The bearing capacity of a circular footing on layered sand under an inclined load depends on the thickness of the dense sand layer (H), the unit weight and friction angle of the upper dense (Υ_1, ϕ_1) and lower loose (Υ_2, ϕ_2) sand layers, the diameter of the footing (D), and the load inclination (α_1) relative to the vertical. It is important to note that the angles α_2, α_3, α_4, and α_5 connected to the load distribution system also depend on the aforementioned parameters. In the present work, in order to obtain a realistic estimate of bearing capacity using the limit equilibrium approach, the magnitude of all load spread angles for surface (α_2, α_3, α_4, and α_5) was estimated by means of finite element analysis in the Plaxis-3D software.

For the numerical investigation, the angle of load inclination (α_1) was applied from 0° to 30° at 10° intervals. In the analysis, the effect of soil density was evaluated. According to [24], the relationship between the unit weights and friction angles utilised for modelling was evaluated for the upper dense and bottom loose sand layers and is shown in Table 1.

Table 1. Soil properties of upper and lower soil layers.

ϕ_1 (Degree)	Υ_1 (kN/m^3)	ϕ_2 (Degree)	Υ_2 (kN/m^3)
41°	19.5	31°	19.5
42°	20	32°	20
43°	20.5	33°	20.5
44°	21	34°	21
45°	21.5	35°	21.5

A numerical study was carried out for various thickness ratios (H/D) ranging from 0.5 to 2.00 [21] provide further information on the numerical investigation. It is important to mention that a finite element analysis was performed on the footing surface. As shown in Figure 3., the failure surface movement varies with load inclination in the form of vectorial surface displacement. Under an inclined load, the failure surface of the circular footing resting on upper dense sand overlying lower loose sand was observed to angle α_2 and α_3 along the loading, but angles α_4 and α_5 were observed to be the same across the loading on the surface footing. Figure 4 shows the load spread angles α_2, α_3, α_4 and α_5 along and across the circular footing's load. As indicated in Figure 4., all load spread angles were measured with respect to the vertical axis in the direction of load inclination. Table 2 illustrates the relationship between the load spread angle (α_1) and the thickness ratio (H/D).

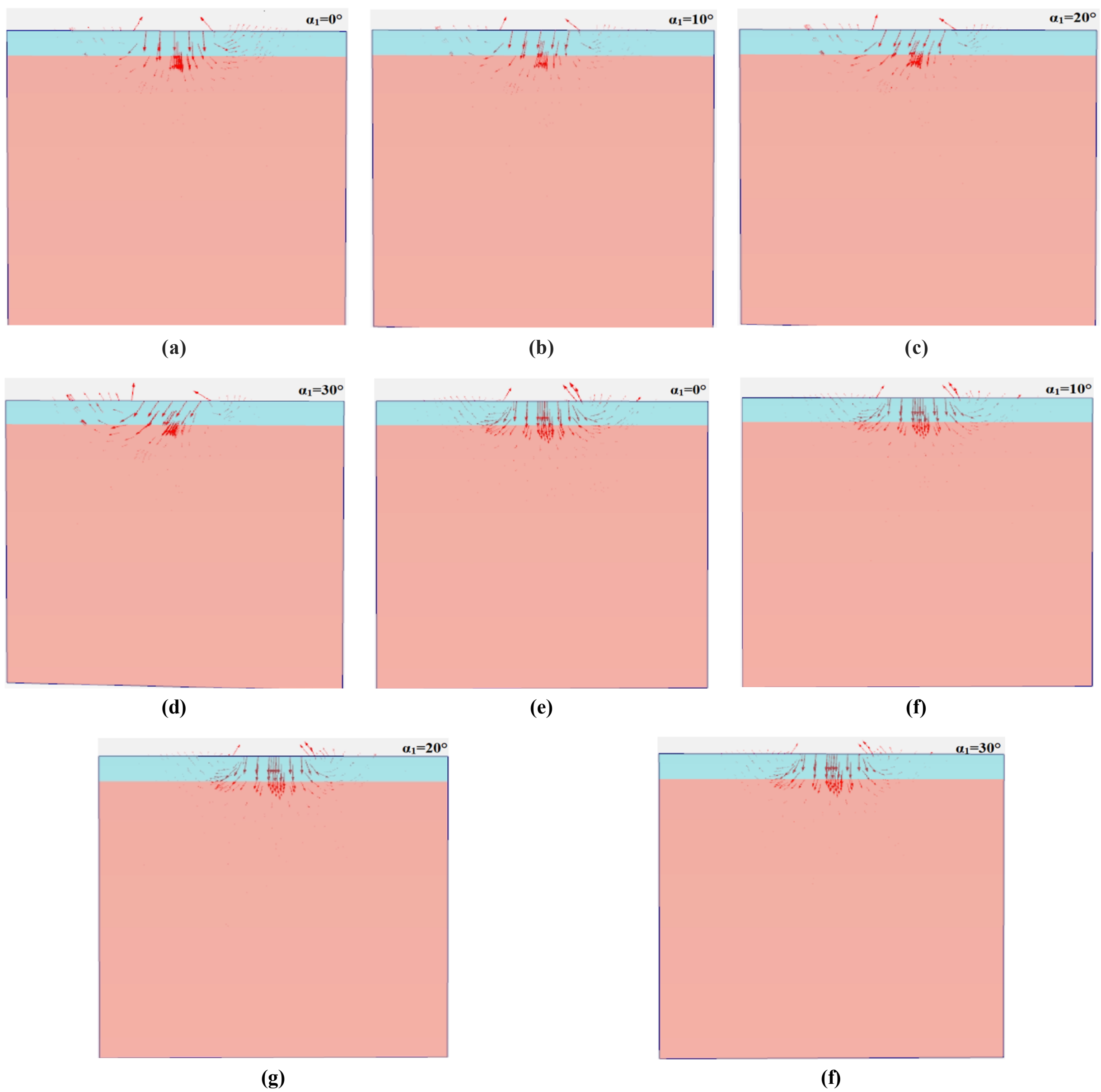

Figure 3. Vectorial displacement failure (a), (b), (c), and (d) along the loading and (e), (f), (g) and (h) across the loading surface footing, under a load inclination of 0° to 30°.

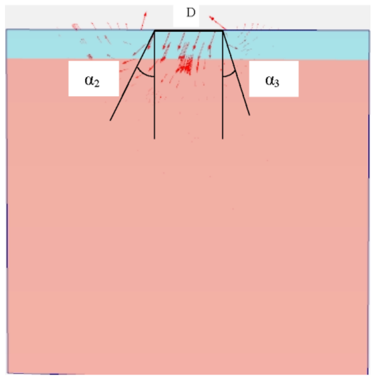

(a)

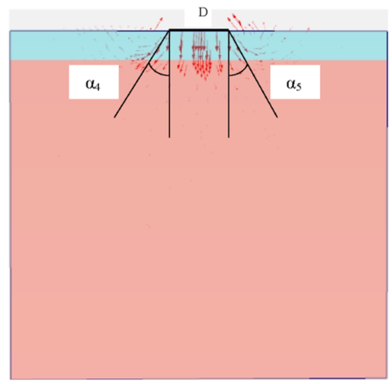

(b)

Figure 4. Load spread angle along and across the loading of the circular footing.

Table 2. Variation of load spread angle with thickness ratio and load inclination.

H/D	α_1 (Deg.)	α_1 at u=0		
		α_2 (Deg.)	α_3 (Deg.)	$\alpha_4 = \alpha_5$ (Deg.)
0.5	0°	10	10	10
1.0		15	15	15
1.5		12	12	12
2.0		10	10	10
0.5	10°	30	-25	10
1.0		20	-30	12
1.5		22	-12	10
2.0		15	-8	15
0.5	20°	45	-30	10
1.0		35	-40	13
1.5		24	-20	10
2.0		28	-24	17
0.5	30°	60	-50	12
1.0		50	-40	14
1.5		35	-30	12
2.0		40	-35	20

Equations describing the surface footing's load spread angle variation with thickness ratio, load inclination, and soil friction ratio were presented as Equation (10). It is important to note that the load spread angles was considered negative when measured to the left of the vertical axis, and positive when measured to the right. For surface footing u=0,

$$\alpha_2 = a\times (H/D) + b \times \alpha_1 + c \times (\phi_2/\phi_1);$$
$$(a = -0.219,\ b = 1.35,\ c = 0.644)$$

$$\alpha_3 = a\times (H/D) + b \times \alpha_1 + c \times (\phi_2/\phi_1); \quad (10)$$
$$(a = -0.157,\ b = 1.085,\ c = 0.0.483)$$

$$\alpha_4 \text{ and } \alpha_5 = a \times (H/D) + b \times \alpha_1 + c\times(\phi_2/\phi_1);$$
$$(a = 0.089,\ b = 0.190,\ c = 0.051)$$

3. Validation using FEM results

In the finite element modelling (FEM) application Plaxis 3d, two layers of a soil model are designed. The model depicts the top layer as consisting of dense sand with a depth of H, the bottom layer as consisting of loose sand with a depth of H' (representing an infinite depth), and D as the diameter of the circular footing. The ratio H/D ranges from 0.5 to 2.0. A circular footing is placed in the centre of the model, and loading is done so in the footing (vertical as well as inclined loading). The horizontal dimensions are maintained so that the boundary effect brought on by loading can be eliminated 5D.

According to [21], a numerical analysis was conducted to calculate the load spread angles α_2, α_3, α_4 and α_5 for the surface footing (u = 0). The proposed Equation (9) is also dependent on these angles of load distribution. Numerical research was undertaken to validate the proposed equation for varied thickness ratios (0.5 to 2.0), load inclination (0° to 30°), and friction angles of the upper dense (41° to 45°) and lower loose (31° to 35°) sand layers under an inclined load. The comparison of the results for the specific parameters of the friction angles, thickness ratio, and load inclination at surface footing was reported in Table 3. Studying Table 3 demonstrates that as the inclination of the load increased from 0° to 30° degrees, the proposed equation yielded identical findings to the finite element analysis. Regarding the FEM results, the average standard deviation was found to be 22.32%, 25.26%, 36.92%, and 45.77% at an angle of 0°, 10°, 20°, and 30° respectively.

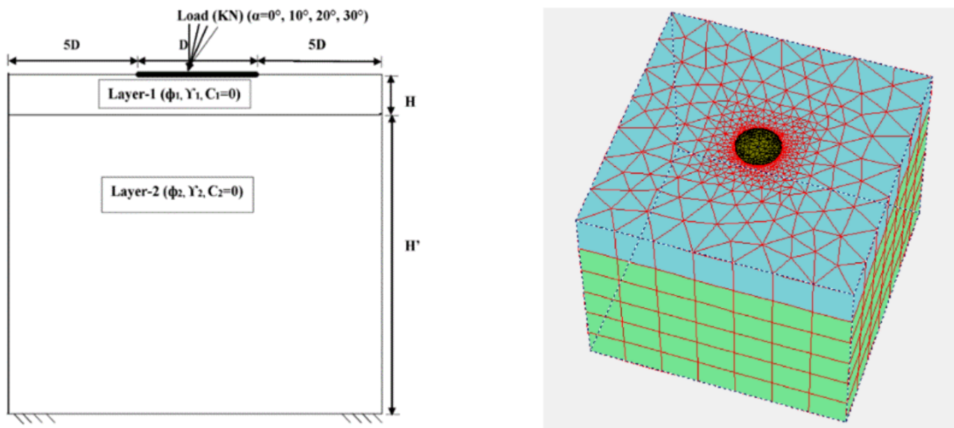

Figure 5. Circular footing resting on layered sand used in the FEM analysis.

The difference between the numerical and mathematical results can be explained by the fact that the bearing capacity found by numerical research matched a peak in the pressure relative settlement plot or was found by the double tangent approach.

4. Results and Discussion

4.1. Effect of thickness ratio and sand friction angle on bearing capacity

In order to evaluate the effect of the thickness ratio and friction angle on the bearing capacity, the results were plotted in Figure 5., corresponding to upper dense friction angles (41° and 45°) and lower loose sand (31°-35°) layer friction angles at varying thickness ratios (0.5 to 2.00) for circular footings subjected to vertical loading. Figure 5. demonstrates that the bearing capacity increased as the thickness ratio increased from 0.5 to 2.0 for the combination of ϕ_1 (41°) and ϕ_2 (31°-35°). It may be due to the increase in thickness of the dense sand layer. In relation, a study of Figure 5 reveals that as the thickness ratio increases, the bearing capacity reaches the value of the upper dense sand's ultimate bearing capacity at a particular thickness ratio and remains constant for the rest of the thickness ratio, with similar behaviour observed for other combinations of thickness ratios. This is due to the fact that, beyond a given thickness ratio, the failure surface remains inside the upper dense sand layer, and no contribution was observed from the bottom loose sand layer. The pattern was the same for all ϕ_1 and ϕ_2 regardless of the thickness ratio. In addition, Figure 5. reveals that corresponding to ϕ_1= 41 and ϕ_2= 31, the surface footing bearing capacity obtained from the proposed equation for a thickness ratio of 0.5 was approximately 312.789 kPa, which increased to 464.980, 718.197, and 1065.830 kPa for thickness ratios of 1.0, 1.5, and 2.0 respectively. It suggests that the bearing capacity for thickness ratios of 1.00, 1.5, and 2 was approximately 0.32, 0.56, and 0.70 times its initial value. Figure 5. demonstrates that as the friction angle of the upper thick sand layer increased from 41° to 45°, the bearing capacity increased due to the rise in frictional resistance. Figure 5. shows that at surface footings with different thickness ratios, the highest and lowest increases in bearing capacity were found for friction angle combinations of 45°-35° and 41°-31°, respectively.

Table 3. Comparison of results with finite element analysis.

H/D	ϕ_1, ϕ_2 (Degree)	Bearing capacity, q_u (kN/m^2)							
		$\alpha_1 = 0^\circ$		$\alpha_1 = 10^\circ$		$\alpha_1 = 20^\circ$		$\alpha_1 = 30^\circ$	
		Present equation	FEM analysis	Present equation	FEM analysis	Present equation	FEM analysis	Present equation	FEM analysis
0.5	41,31	312.79	270	164.794	182	79.27243	125	46.74	75
1.0		464.98	350	310.250	330	202.5139	225	154.82	175
1.5		719.20	650	559.091	585	429.4591	440	326.41	310
2.0		1065.83	985	825.316	850	551.8388	580	415.29	445
0.5	43,31	329.32	305	179.875	220	93.43018	160	59.63	105
1.0		517.73	480	360.048	385	246.4229	260	193.94	215
1.5		830.29	790	666.020	680	525.6027	545	405.52	435
2.0		1255.31	1190	993.144	1050	677.5468	705	516.47	545
0.5	45,31	349.69	345	198.483	245	110.9013	175	75.53	120
1.0		582.50	540	421.207	440	300.3808	330	242.02	265
1.5		966.43	920	797.065	820	643.4652	665	502.56	530
2.0		1487.24	1390	1198.671	1245	831.6684	845	640.61	675
0.5	41,32	343.06	310	183.498	190	86.11809	132	47.40	82
1.0		495.25	450	328.954	350	209.3596	240	155.48	180
1.5		749.47	720	577.795	610	436.3047	460	327.07	340
2.0		1096.10	1040	844.020	875	558.6845	590	415.95	450
0.5	43,32	359.59	350	198.580	235	100.2758	165	60.28	108
1.0		548.00	515	378.752	410	253.2686	275	194.59	220
1.5		860.56	820	684.724	715	532.4483	560	406.18	445
2.0		1285.58	1220	1011.849	1060	684.3925	720	517.12	550
0.5	45,32	379.96	380	217.187	255	117.7469	180	76.19	124
1.0		612.77	565	439.912	450	307.2265	335	242.67	270
1.5		996.70	935	815.769	830	650.3109	670	503.22	535
2.0		1517.51	1440	1217.375	1260	838.514	860	641.27	680
0.5	41,33	424.06	390	224.002	205	100.9256	138	48.73	85
1.0		576.25	530	369.458	380	224.167	245	156.81	185
1.5		830.47	780	618.299	630	451.1122	475	328.40	350
2.0		1177.10	1120	884.524	910	573.492	615	417.28	460
0.5	43,33	440.59	415	239.083	260	115.0833	170	61.61	110
1.0		629.00	585	419.256	440	268.076	285	195.92	235
1.5		941.56	860	725.228	740	547.2558	585	407.51	450
2.0		1366.58	1280	1052.352	1080	699.2	735	518.46	560
0.5	45,33	460.96	450	257.691	280	132.5544	190	77.52	125
1.0		693.77	625	480.415	490	322.034	340	244.00	275
1.5		1077.70	1020	856.273	840	665.1183	675	504.55	545
2.0		1598.51	1520	1257.879	1280	853.3215	870	642.60	685
0.5	41,34	462.64	425	245.888	265	111.1597	145	50.46	88
1.0		614.83	580	391.344	425	234.4012	264	158.55	190
1.5		869.05	815	640.185	650	461.3464	485	330.13	365
2.0		1215.68	1180	906.410	925	583.7261	630	419.01	475
0.5	43,34	479.17	450	260.970	295	125.3175	172	63.35	112
1.0		667.58	625	441.142	460	278.3102	290	197.66	240
1.5		980.14	935	747.114	775	557.49	590	409.24	460
2.0		1405.16	1360	1074.239	1110	709.4341	745	520.19	565
0.5	45,34	499.54	495	279.577	315	142.7886	194	79.26	128
1.0		732.35	705	502.301	520	332.2681	350	245.74	280
1.5		1116.28	1080	878.159	890	675.3525	690	506.29	550
2.0		1637.09	1585	1279.765	1320	863.5557	890	644.33	690
0.5	41,35	537.45	510	290.746	330	128.1978	150	53.69	90
1.0		689.64	625	436.201	455	251.4393	274	161.77	192
1.5		943.86	910	685.043	710	478.3845	505	333.36	370
2.0		1290.49	1230	951.267	965	600.7642	635	422.24	480
0.5	43,35	553.98	540	305.827	350	142.3556	175	66.58	114
1.0		742.40	710	485.999	515	295.3483	325	200.89	245
1.5		1054.95	1005	791.971	830	574.528	605	412.47	465
2.0		1479.97	1435	1119.096	1140	726.4722	750	523.42	570
0.5	45,35	574.35	565	324.435	360	159.8267	198	82.49	130
1.0		807.17	775	547.159	580	349.3062	375	248.97	285
1.5		1191.09	1125	923.016	945	692.3906	725	509.52	560
2.0		1711.91	1660	1324.623	1350	880.5937	935	647.56	695

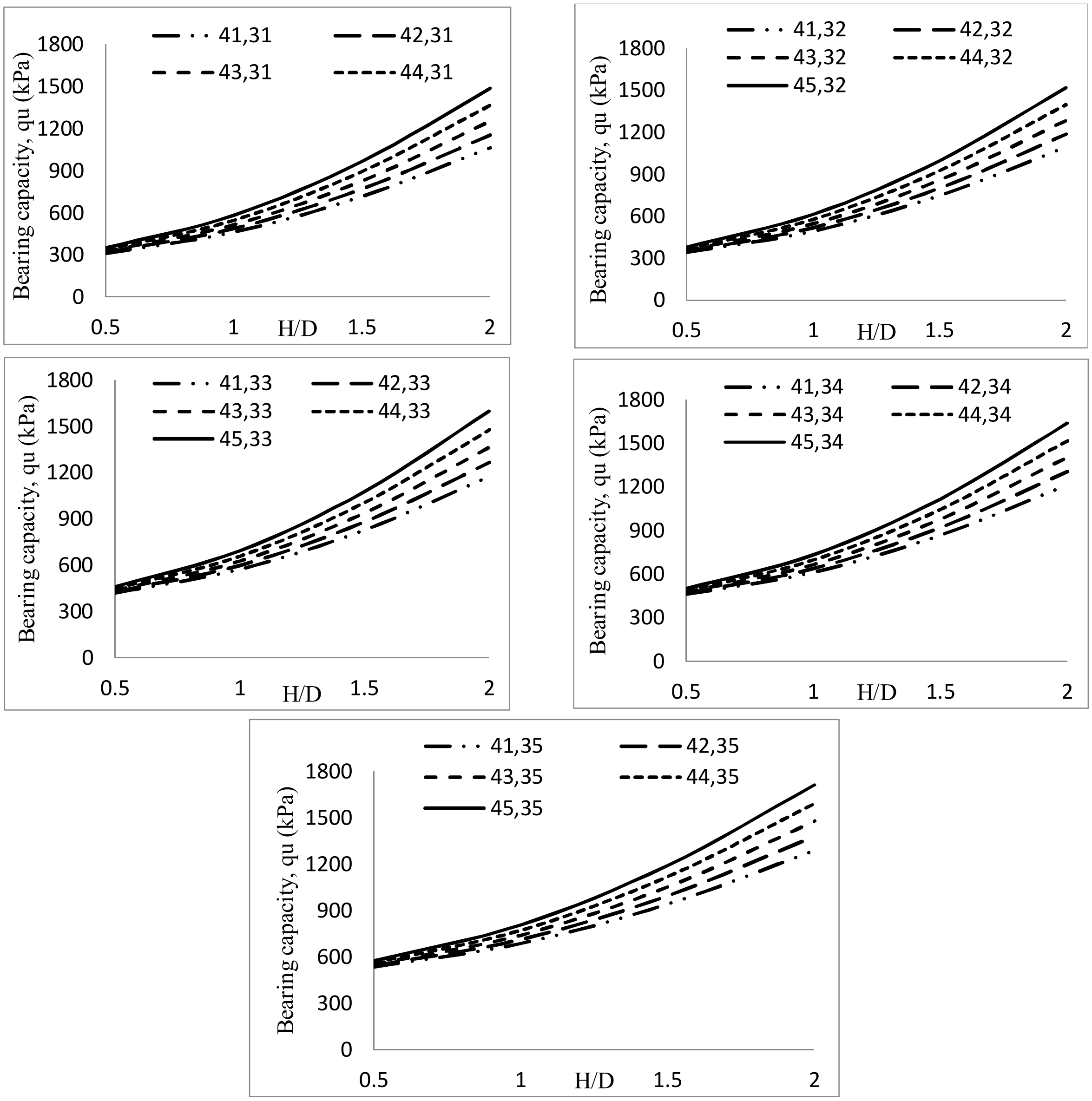

Figure 6. Plot of bearing capacity of surface circular footing with varying ϕ_1 (41°-45°) and ϕ_2 (31°-35°) at varying thickness ratio.

4.2. Effect on load inclination on bearing capacity

In order to examine the effect of load inclination on bearing capacity, the results for upper dense sand friction angle (41° to 45°) and lower loose sand friction angle (31° and 35°) at varying load inclination (0° to 30°) for thickness ratio (H/D = 0.5 and 2.0) at surface footing were plotted in Figure 6. Figure 6. demonstrates that at thickness ratios of 0.5 and 2.0, as the load inclination increases from 0° to 30°, the bearing capacity decreases for all friction angle combinations. This may be attributed to the displacement of the failure surface in the direction of load application. Additionally, the vertical and horizontal displacements were observed to decrease and increase, respectively, resulting in footing failure. With ϕ_1= 41° and ϕ_2= 31° and a thickness ratio of 0.5, the bearing capacity of surface footing determined from the proposed equation for a load inclination of 0° was about 312.786 kPa, which decreased to 164.794, 79.272 and 46.739 kPa for load inclinations of 10°, 20°, and 30°, respectively. It indicates that the bearing capacity at a load inclination of 10°, 20°, and 30° decreased by 47.31%, 74.66%, and 85.06% of its initial value, respectively.

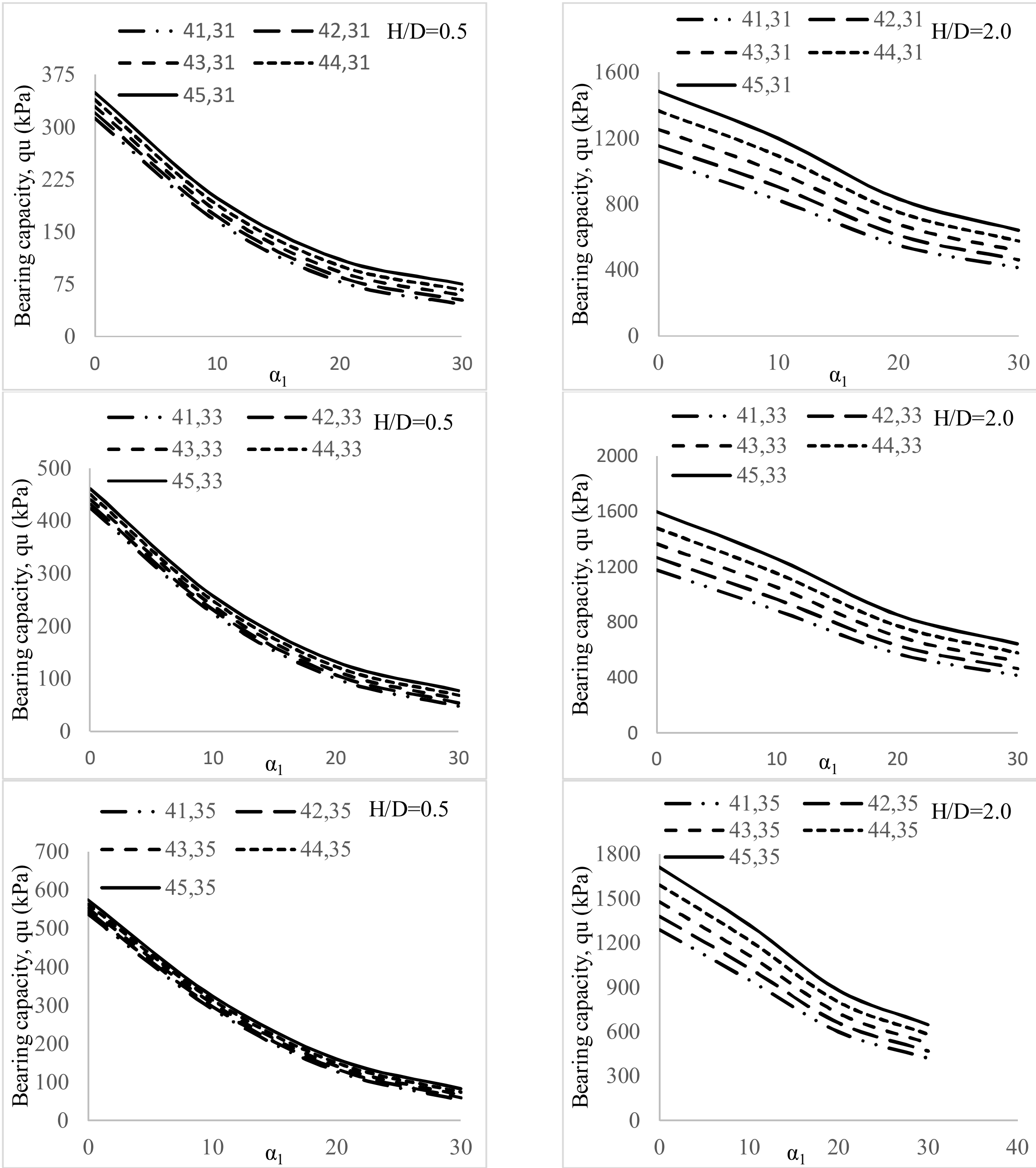

Figure 7. Plot of bearing capacity at surface footing with varying load inclination (α_1= 0° to 30°) for soil combination of ϕ_1 (41°-45°) and ϕ_2 (31°, 33° and 35°) at thickness ratio of 0.5 and 2.0.

4.3. Comparison

The experimental results provided by [2] were compared with the equation's predicted results (9). The bearing capacity derived from equation (9) was calculated and compared to the results provided by [2] for circular footing. [2] determined the friction angle and unit weight of the upper dense and lower loose sand layers to be 47.5° and 34°, 16.33 kN/m^3 and 13.78 kN/m^3, respectively. The comparison was represented in Figure 7. for a load inclination of 0°, 10°, 20°, and 30° for varied surface thickness ratios (H/D). In comparison to [2] results, Figure 7. demonstrates that the values obtained from the suggested Equation (9) at smaller thickness ratios are conservative. For greater thickness ratios (> 0.5), the results obtained from the suggested Equation (9) were greater than those obtained from [2]. In comparison to the results given by [2], the average deviation in the results derived from the proposed equation (9) was around 62%, 50 %, 36 %, and 36 % for thickness ratio H/D = 0.5 when the load inclination was 0°, 10°, 20° and 30° . All variations may be explained by the fact that [2] expected the load spread angle to be equal to the angle of load inclination.

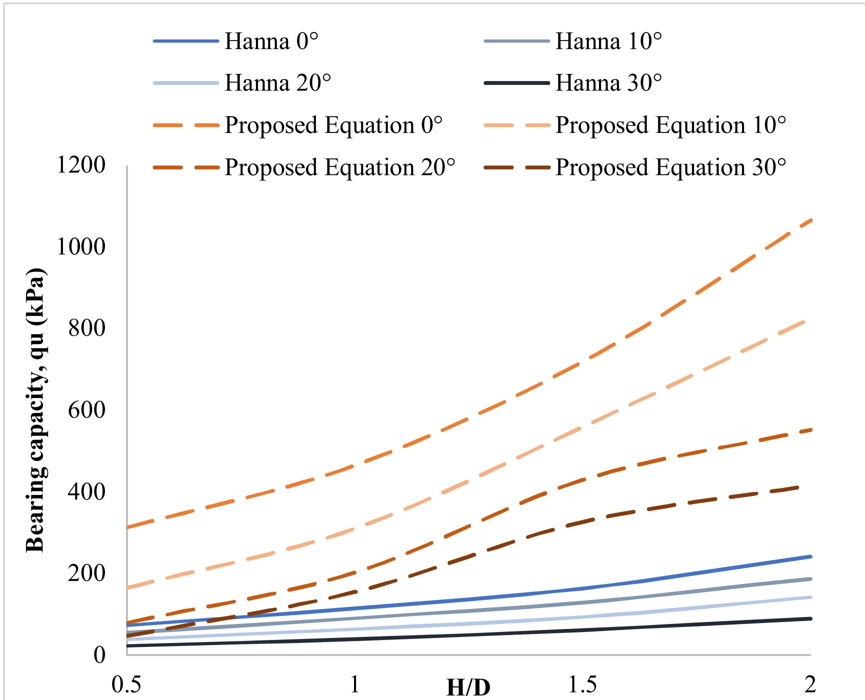

Figure 8. Comparison of the circular footing at the surface with the literature.

5. Conclusions

In this work, the bearing capacity equation for a circular footing subjected to an inclined load and resting on layered sand (dense sand overlying loose sand) was derived using a well-known limit equilibrium methodology in combination with the load spread mechanism. The results of this investigation led to the following conclusions:

1. At different thickness ratios, the bearing capacity increased the most when the friction angle was 45°-35° and the least when it was 41°-31°.

2. For $\phi_1 = 41^\circ$ and $\phi_2 = 31^\circ$, and a thickness ratio of 0.5 and 2.00, the bearing capacity at a load inclination of 0°, 10°, 20°, and 30° decreased by approximately 47.31%, 74.66%, 85.06%, and 22.57%, 48.22%, 61.04% of its initial value, respectively.

3. With $\phi_1 = 45^\circ$ and $\phi_2 = 35^\circ$, and a thickness ratio of 0.5 and 2.00, the bearing capacity at a load inclination of 0°, 10°, 20°, and 30° decreased by approximately 43.51%, 72.17%, 85.64%, and 22.62%, 48.56%, 62.17% of its initial value, respectively.

4. Compared to the proposed equation estimations, the average deviation for load inclination values of 0°, 10°, 20°, and 30° was 7%, 5%, 22%, and 23% for finite element results.

5. The results obtained from the proposed bearing capacity equation were found to be equivalent to those reported in the literature, with average deviations of 62%, 50%, 36%, and 36% for load inclination values of 0°, 10°, 20°, and 30°, respectively.

List of symbols

ϕ_1, ϕ_2	Soil friction angle for upper dense sand and Lower loose sand soil, in degree
γ_1, γ_2	Unit weight of the upper dense sand soil and lower loose sand soil, kN/m^3
α_2, α_3, α_4, and α_5	Load spread angles along and across the diameter of the footing, in degree
E_1,E_2	Elastic moduli for upper dense sand and lower loose sand layer
υ_1, υ_2	Poisons ratio for upper layer and lower layer
D	Diameter of the footing
dz	Small strip Thickness
α_1	Concentric load inclination angle with respect to vertical acting on the circular footing, in degree
σ	Stress applied on the footing, kN/m^2
H	Thickness of the upper dense sand layer
u	Depth of the embedded footing from ground surface
P_p	Total passive earth pressure acting normal to the failure plane
dP_{pv}	Small passive earth pressure acting on small strip soil in vertical direction
K_p	Passive earth pressure coefficient
q_u or q_{uv} cos α_1	Ultimate load bearing capacity of the rectangular footing in the layered sand (vertical component)
q_b	Ultimate bearing capacity of lower loose sand
i_q , i_Υ	Inclination factors
S_γ, S_q	Shape factors
N_q, N_γ	Bearing capacity
d_q, d_γ	Depth factors
c	Constant of integration
δ	Mobilised shearing resistance angle at failure, degree
z	Distance where small strip of soil lies below circular footing
H/D	Thickness ratio
ϕ_2/ϕ_1	Soil friction ratio

Acknowledgement

The authors are grateful to the CSIR-CBRI Roorkee, Uttarakhand, India, for providing to utilize the Plaxis-3D software for this work.

Funding:

The authors received no monetary compensation of any kind.

Conflict of Interest:

The authors have no conflict of interest with any one, and are related to the material presented in the paper.

References

[1]. Meyerhof, G.G. and Hanna, A.M. (1974). Ultimate Bearing Capacity of Foundation on Layered Soils Under Inclined Load. Can Geotech Journal. 15 (4): 565–72.

[2]. Meyerhof, G.G. and Hanna, A.M. (1978). Ultimate Bearing Capacity of Foundations on Layered Soils Under Inclined Load. Can Geotech Journal. 15 (4): 565–72.

[3]. Hanna, A.M. (1981). Foundation on Strong Sand Overlying Weak Sand. J Geotech Engrg Div.107(7): 915–27.

[4]. Michalowski, R.L. and Shi, L. (1995). Bearing capacity of footings over two-layer foundation soils. J Geotech Eng. 121 (5): 421–8.

[5]. Al-Adly, A.I.F., Fadhil, A.I. and Fattah, M.Y. (2019). Bearing capacity of isolated square footing resting on contaminated sandy soil with crude oil. Egypt J Pet [Internet]. 28 (3): 281–8. Available from: https://doi.org/10.1016/j.ejpe.2019.06.005

[6]. Das, P.P. and Khatri, V.N. (2020). Bearing capacity estimation of shallow foundations on dense sand underlain by loose sand strata using finite elements limit analysis. Lect Notes Civ Eng. 84, 203–14.

[7]. Gupta, S. and Mital, A. (2022). A comparative study of bearing capacity of shallow footing under different loading conditions. Geomech Geoengin [Internet]. 17 (4): 1338–49. Available from: https://doi.org/10.1080/17486025.2021.1940310

[8]. Khatri, V.N., Kumar, J. and Akhtar, S. (2017). Bearing capacity of foundations with inclusion of dense sand layer over loose sand strata. Int J Geomech. 17(10): 1–8.

[9]. Das, P.P., Khatri, V.N. and Kumar, J. (2022). Bearing capacity of strip and circular footing on layered sand with geogrid at the interface. Arab J Geosci [Internet]. 15 (4): 1–13. Available from: https://doi.org/10.1007/s12517-022-09614-1

[10]. Joshi, V.C., Dutta, R.K.and Shrivastava, R.

(2015). Ultimate bearing capacity of circular footing on layered soil. J Geoengin. 10 (1): 25–34.

[11]. Okamura, M., Takemura, J.and Kimura, T. (1998). Bearing capacity predictions of sand overlying clay based on limit equilibrium methods. Soils Found. 38 (1): 181–94.

[12]. Kumar, A., Ohri, M.L.and Bansal, R.K. (2007). Bearing capacity test of strip footings on reinforced layered soil. Geotech Geol Eng. 25 (2): 139–50.

[13]. Nikraz, H.M.A. (2015). Bearing Capacity Evaluation of Footing on a Layered-Soil using ABAQUS. J Earth Sci Clim Change. 06 (03).

[14]. Misir, G.and Laman, M. (2017). A modern approach to estimate the bearing capacity of layered soil. Period Polytech Civ Eng. 61 (3): 434–46.

[15]. Kumar, V.S.K.R.D.T.K (2018). Behaviour of Foundation in Layered Soils. Int J Sci Res [Internet]. 7(1): 1075–8. Available from: https://www.ijsr.net/archive/v7i1/ART20179556.pdf

[16]. Shoaei, M.D., Alkarni, A., Noorzaei, J., Jaafar, M.S.and Huat, B.B.K. (2012). Review of available approaches for ultimate bearing capacity of two-layered soils. J Civ Eng Manag. 18 (4): 469–82.

[17]. Rao, P., Liu, Y., and Cui, J. (2015). Bearing capacity of strip footings on two-layered clay under combined loading. Comput Geotech [Internet]. 69, 210–8. Available from: http://dx.doi.org/10.1016/j.compgeo.2015.05.018

[18]. Al-Ameri, A.F., Hussein, S.A., and Mekkiyah, H. (2020). Estimate the bearing capacity of full-scale model shallow foundations on layered-soil using Plaxis. Solid State Technol [Internet]. 63 (1): 1775–87.

[19]. Tajeri, S., Sadrossadat, E., and Bazaz, J.B. (2015). Indirect estimation of the ultimate bearing capacity of shallow foundations resting on rock masses. Int J Rock Mech Min Sci [Internet]. 80,107–17. Available from: http://dx.doi.org/10.1016/j.ijrmms.2015.09.015

[20]. Panwar, V.and Dutta, R.K. (2021). Bearing capacity of rectangular footing on layered sand under inclined loading. J Achiev Mater Manuf Eng. 108 (2): 49–62.

[21]. Singh, S.P.and Roy, A.K. (2021). Numerical Study of the Behaviour of a Circular Footing on a Layered Granular Soil Under Vertical and Inclined Loading. Civ Environ Eng Reports. 31 (1): 29–43.

[22]. Alavi, A.H.and Sadrossadat, E. (2016). New design equations for estimation of ultimate bearing capacity of shallow foundations resting on rock masses. Geosci Front [Internet]. 7 (1): 91–9. Available from: http://dx.doi.org/10.1016/j.gsf.2014.12.005

[23]. BIS:6403 (1981). Code of Practice for Determination of Breaking Capacity of Shallow Foundations. Bur Indian Stand New Delhi.

[24]. Bowles, J.E. (1977). Foundation analysis and design. New York: McGraw-Hill.

فرموله کردن معادله ظرفیت باربری برای یک پایه دایره‌ای با بارهای عمودی و شیب‌دار بر روی ماسه لایه‌ای

سوریا پراتاپ سینگ* و امریت کومار روی

گروه مهندسی عمران، NIT Hamirpur، هیماچال پرادش، هند

ارسال ۲۰۲۲/۱۰/۰۹، پذیرش ۲۰۲۲/۱۲/۱۱

* نویسنده مسئول مکاتبات: surya_phdce@nith.ac.in

چکیده:

این کار تحقیقاتی معادله ظرفیت باربری را برای یک پایه دایره‌ای که بر روی ماسه متراکم پوشانده شده و تحت بارگذاری عمودی و شیب‌دار قرار می‌گیرد، با استفاده از تعادل حدی به دنبال رویکرد منطقه پیش‌بینی‌شده، ارائه می‌کند. برای مطالعه پارامتری، متغیرها شامل نسبت ضخامت لایه ماسه متراکم بالایی (۰٫۵ تا ۲٫۰۰)، زاویه اصطکاک ماسه متراکم بالایی (۴۱ درجه تا ۴۵ درجه) و لایه ماسه سست پایین (۳۱ درجه تا ۳۵ درجه)، و تمایل بار اعمال شده است. (۰ تا ۳۰ درجه) بیشترین و کمترین افزایش ظرفیت باربری به ترتیب برای ترکیب‌های زاویه اصطکاک ۴۵-۳۵ درجه و ۴۱-۳۱ درجه برای نسبت‌های مختلف ضخامت گزارش شده است. برای شیب‌های بار ۰ درجه، ۱۰ درجه، ۲۰ درجه و ۳۰ درجه، ظرفیت باربری ۴۳/۵۱٪، ۷۲/۱۷٪، ۸۵/۶۴٪، و ۲۲/۶۲٪، ۴۸/۵۶٪، ۶۲/۱۷٪ برای زوایای اصطکاک ماسه سست متراکم بالا و پایین کاهش می‌یابد. ترکیب لایه‌های ۴۵ درجه و ۳۵ درجه و با نسبت ضخامت ۰/۵ و ۲ با در نظر گرفتن نتایج المان محدود، میانگین انحراف ظرفیت باربری حاصل از معادله پیشنهادی در پایه سطحی برای شیب های بار ۰ درجه، ۱۰ درجه، ۲۰ درجه و ۳۰ درجه به ترتیب ۷٪، ۵٪، ۲۲٪ و ۲۳٪ است. معادله ظرفیت باربری پیشنهادی نتایجی را به دست می‌دهد که با میانگین انحرافات ۶۲، ۵۰، ۳۶ و ۳۶ درصد به ترتیب برای مقادیر شیب بار ۰ درجه، ۱۰ درجه، ۲۰ درجه و ۳۰ درجه، با مقالات موجود مقایسه شد.

کلمات کلیدی: پایه دایره‌ای، رویکرد منطقه پیش‌بینی شده، بارگذاری عمودی و شیبدار، ماسه لایه‌ای.